



OPEN ACCESS

EDITED BY

Honglei Sun,
Zhejiang University of Technology, China

REVIEWED BY

Maria Cruz Alonso,
Spanish National Research Council
(CSIC), Spain
Chuanqing Fu,
Zhejiang University of Technology, China
Chunping Gu,
Zhejiang University of Technology, China

*CORRESPONDENCE

Linjian Wu

✉ wljabgf@126.com

Mingwei Liu

✉ mingwei_liu@126.com

RECEIVED 17 December 2023

ACCEPTED 02 April 2024

PUBLISHED 25 April 2024

CITATION

Jiang H, Wu L, Guan L, Liu M, Ju X, Xiang Z,
Jiang X, Li Y and Long J (2024) Durability
life evaluation of marine infrastructures
built by using carbonated recycled coarse
aggregate concrete due to the chloride
corrosive environment.
Front. Mar. Sci. 11:1357186.
doi: 10.3389/fmars.2024.1357186

COPYRIGHT

© 2024 Jiang, Wu, Guan, Liu, Ju, Xiang, Jiang,
Li and Long. This is an open-access article
distributed under the terms of the [Creative
Commons Attribution License \(CC BY\)](https://creativecommons.org/licenses/by/4.0/). The
use, distribution or reproduction in other
forums is permitted, provided the original
author(s) and the copyright owner(s) are
credited and that the original publication in
this journal is cited, in accordance with
accepted academic practice. No use,
distribution or reproduction is permitted
which does not comply with these terms.

Durability life evaluation of marine infrastructures built by using carbonated recycled coarse aggregate concrete due to the chloride corrosive environment

Han Jiang¹, Linjian Wu^{1*}, Li Guan², Mingwei Liu^{1*}, Xueli Ju¹,
Zhouyu Xiang¹, Xiaohui Jiang¹, Yingying Li¹ and Jia Long¹

¹National Engineering Research Center for Inland Waterway Regulation, School of River and Ocean Engineering, Chongqing Jiaotong University, Chongqing, China, ²First Design Branch of Water Transport, Sichuan Communication Surveying & Design Institute Co. Ltd., Chengdu, China

Due to the harsh marine environment of chloride ion invasion and corrosion, the issues of long-term chloride transport and durability life evaluation for marine infrastructures constructed/maintained by recycled aggregate concrete (RAC) after enhancement remain poorly understood. For our studies, an accelerated carbonation modification method for recycled coarse aggregate (RCA) was adopted to prepare carbonated recycled coarse aggregate (CRCA) samples, and the macroproperties, i.e., apparent density and water absorption, of CRCA were enhanced by approximately 1.40-3.97% and 16.3-21.8%, respectively, compared with those of RCA. An in-door experiment for chloride transport into concrete specimens subjected to a simulated marine environment of alternating drying-wetting cycles was conducted. The chloride profiles and transport characteristics of carbonated recycled coarse aggregate concrete (CRCAC), recycled coarse aggregate concrete (RCAC), and natural coarse aggregate concrete (NCAC) were analysed and compared. The results indicated that the chloride penetration depths and concentrations of CRCAC were approximately 52.6-96.2% of those of RCAC, which highlighted the better chloride resistance of CRCAC. A chloride transport model for marine concrete structures with various coarse aggregate types in a corrosive marine environment was established. Taking a certain harbour wharf as an example, the durability life of this case considering the application of the CRCAC was evaluated based on the chloride transport model, and the durability life of the CRCAC structure was improved by approximately 28.10% compared with that of the RCAC. The CRCAC developed in this paper has improved mechanical performance and durability than those of RCAC, and it has the potential to replace the NCAC and further support the construction and maintenance of marine infrastructures.

KEYWORDS

marine infrastructures, carbonated recycled coarse aggregate concrete (CRCAC), marine corrosive environment, chloride transport, structural durability evaluation

1 Introduction

Oceans have received considerable attention for their abundant energy, mineral, and biological resources, making the development of marine infrastructures critical for the efficient exploitation of these resources (Bangley et al., 2022). Marine infrastructures include harbours, seawalls, offshore wind farms, offshore pipelines, tidal stream turbines, oil and gas platforms, cross-sea bridges, subsea tunnels, and so on (Guo et al., 2023). The construction, operation and development of marine infrastructures consume a large amount of the raw materials of reinforced concrete (RC) (He and Lu, 2023). In the face of the current major strategic requirements for the construction and development of marine infrastructures, as well as the increasing shortages of natural resources, such as aggregates of sand and crushed stone, for producing concrete worldwide, the promotion and utilization of waste concrete to produce/prepare recycled aggregate (RA) and recycled aggregate concrete (RAC) (Feng et al., 2022; Zhang et al., 2022) and the further treatment of these materials as concrete raw materials for RC structures of marine infrastructures must be the general trend in the future. This initiative can not only greatly reduce carbon emissions and decrease the exploitation of natural resources but also effectively promote the protection of the marine ecological environment, which has become a hot topic in the field of structures and materials in marine infrastructures worldwide.

However, the mechanical strength and durability (resistance to chloride penetration) of RA and its RAC used in marine

infrastructures are worse than those of the natural aggregate and its concrete due to numerous pores and microcracks within the old mortar (OM) and the old interfacial transition zone (OITZ) of RA, as well as the formative multiple mesoscopic interface structure of RAC (see Figure 1). The microstructure of ITZ is shown in Figure 1C (Liang et al., 2019) and Figure 1D (Li et al., 2020). On the basis of this figure, the ITZ within the RCAs before accelerated carbonation is loose and has obvious cracks. In accordance with Wang et al. (2016), the OM and OITZ of RA contain a series of components, including calcium silicate hydrate (C-S-H), calcium hydroxide ($\text{Ca}(\text{OH})_2$), unhydrated C_3S , C_2S , etc. Carbon dioxide (CO_2) can chemically react with these components and further form dense CaCO_3 and silica gel ($\text{SiO}_2 \cdot n\text{H}_2\text{O}$), resulting in an increase in the solid phase volumes of the generated products of approximately 11–12% compared with the original components (Liang et al., 2020); this can further decrease the pores and microcracks within the OM and the OITZ of the RA and improve the microstructure of the RA, thereby enhancing the properties of the RA and its RAC (Tam et al., 2020; Hosseini Zadeh et al., 2021; Pu et al., 2021).

In addition, the issues of marine structural performance deterioration, long-term durability and reliability for coastal reinforced concrete (RC) infrastructures caused by chloride ion invasion exposed to marine environments (Das and Pradhan, 2023; Lai et al., 2023; Prusty and Pradhan, 2023; Wally et al., 2023; de Vera et al., 2024) can seriously restrict the practical application of RA and its RAC for construction and development in marine engineering. Therefore, the property enhancement of RA and its



FIGURE 1 Mesoscopic structure of the (A) RA, (B) RAC, and (C) microstructure of the ITZ (Liang et al., 2019) and (D) microstructure of the ITZ (Li et al., 2020).

RAC, as well as the long-term durability of modified RAC prepared from RA after modification, are considered vital issues that must be urgently researched and resolved to promote the application of RA and its RAC in marine infrastructures.

For RC structures exposed to marine environments, especially those exposed to marine zones with alternating drying-wetting cycles, chloride ion invasion into concrete via multiple transmission mechanisms, including diffusion, convection, etc., is generally considered the vital reason for rebar corrosion, which can risk the long-term durability and reliability of RC structures to a great extent (Gao et al., 2019; Shen et al., 2019; Ashrafian et al., 2022). Many classical studies have reported the transport of chloride ions into fresh natural aggregate concrete composites (Bao et al., 2022; Ou et al., 2022; Gašpárek et al., 2023; Pontes et al., 2023; Qian et al., 2023; de Vera et al., 2024; Korec et al., 2024). However, the RAC contains a new ITZ (NITZ) and an OITZ structure, and the large number of pores and cracks as well as the unhydrated cement particles are included in the NITZ and OITZ; hence, they are regarded as the weakest link within RAC, which can greatly reduce its resistance to chloride ion penetration (Liang et al., 2019). Moreover, the multiple interface structural characteristics of RAC can increase the connectivity of its internal pores and microcracks (Ortolan et al., 2023; Pandey and Rajhans, 2023), which results in chloride ion transport behaviours in RAC that are more complex than those in natural aggregate concrete (NAC) (Sua-iam and Makul, 2024).

However, there are few published reports on long-term chloride ion transport characteristics and durability evaluations for marine infrastructures constructed using recycled aggregate concrete based on carbonated recycled aggregate (CRA) exposed to marine environments. The stability and durability of marine infrastructures built from carbonated recycled aggregate concrete (CRAC) in operation remain poorly understood. Consequently, studying the risks and reliability of CRAC structures exposed to marine environments is critical for providing practical insights into protecting the stable operation of marine infrastructures. In summary, to further promote the application of CRA and its CRAC in marine infrastructures, the corresponding key durability issues for CRAC structures, including chloride profiles, transport characteristics and computational models, as well as structural durability evaluations under marine environments, need to be addressed.

In our study, two significant aspects, i.e., chloride transport in carbonated recycled coarse aggregate concrete (CRCAC) and durability evaluation of marine infrastructures using CRCAC in marine drying-wetting environments, were considered. During this paper's investigations, sufficient carbonated recycled coarse aggregate (CRCA) samples with different particle diameters based on the gaseous CO₂ accelerated carbonation method were acquired. Subsequently, the chloride profiles and transport characteristics of concrete cast by various coarse aggregate types, including natural coarse aggregate concrete (NCAC), recycled coarse aggregate concrete (RCAC) and CRCAC, subjected to a simulated marine environment with alternating drying-wetting cycles were analysed and compared. A computational model of chloride transport in concrete considering coarse aggregate types under a marine drying-

wetting alternating environment was established, which can be used to estimate the long-term chloride transport behaviours of different concrete types (NCAC, RCAC, and CRCAC), especially for CRCAC. Finally, using the chloride transport computational model proposed in this paper, the durability life of marine infrastructure (an example of a certain harbour wharf) considering the application of the CRCAC was evaluated.

In summary, the significant research contents, objectives and innovations for this paper are highlighted as follows:

- (1) An accelerated carbonation modification method for RCAs is adopted to prepare the CRCA, which can effectively enhance the properties of RCAs after accelerated carbonation.
- (2) An in-door experiment for chloride transport into concrete cast by various coarse aggregate types under a simulated marine environment of alternating drying-wetting cycles is conducted, and the chloride profiles and transport characteristics of the NCAC, RCAC and CRCAC are described.
- (3) A chloride transport model for marine concrete structures with various coarse aggregate types in a corrosive marine environment is established, and the durability life of a certain harbour wharf hypothetically constructed by the CRCAC is evaluated based on this chloride transport model.

2 Materials and methodology

2.1 Materials

Composite silicate cement, i.e., PC.42.5R, natural crush stones with a particle diameter range of 5–20 mm and continuous grading, freshwater river sand with a fineness modulus of 2.6 and continuous grading, and drinking water with a density of $\rho_w=1 \text{ g/cm}^3$ were used as the raw materials for casting and preparing sufficient original C40-strength concrete specimens (100×100×100 mm³ cube) based on the Chinese standard (JTJ 270-1998, 1998). The mix proportions for the C40-strength concrete specimens are listed in Table 1, and the particle grading distributions of the aggregates in the concrete specimens, including the coarse aggregates and fine aggregates, are shown in Supplementary Figure 1.

All C40-strength concrete specimens were cast in plastic moulds and subsequently compacted using a vibrating table. After 24 h of curing at 20 ± 5°C and a relative humidity of approximately 50–55%, the concrete specimens were demoulded and transferred to saturated Ca(OH)₂ solutions for 28 days of ageing, and the environmental temperature was set to 20 ± 3°C.

Samples of RCAs with various particle diameters of 5–10 mm, 10–20 mm, and 20–25 mm were acquired through crushing and sieving from the aforementioned original C40-strength concrete specimens by using a crusher (see Supplementary Figure 2A and Taylor sieve machine (see Supplementary Figure 2A)). These prepared RCA samples were subsequently used for the accelerated carbonation experiment (ACE) of the RCAs.

TABLE 1 Mix proportions of the original concrete for RCA preparation.

w/c	Cement (kg/m ³)	Water (kg/m ³)	Fine aggregate (kg/m ³)	Coarse aggregate (kg/m ³)
0.5	390	195	617	1198

Moreover, natural coarse aggregate (NCA) samples with identical particle diameters of 5-10 mm, 10-20 mm, and 20-25 mm were acquired by utilizing the identical sieving method of RCA. The prepared samples of recycled coarse aggregate (RCA) and NCA were placed in a drying oven at a constant temperature of 105 ± 5°C for more than 24 h until they reached a constant weight (Wu et al., 2023; Yang et al., 2023; Ju et al., 2024), after which they were removed and cooled to the general temperature for subsequent tests, including the ACE of the RCA and initial property measurements of the RCA and NCA.

2.2 Methodology

2.2.1 Preparation of CRCA based on the accelerated carbonation method

The ACE for the RCA samples with various particle diameters based on the accelerated carbonation method was determined by using a carbonation chamber for the cement-based composites, as shown in Supplementary Figure 3A. The environmental temperature (ET), relative humidity (RH), and CO₂ concentration were set as constants of 20 ± 2°C, 70 ± 5%, and 20 ± 3%, respectively, inside the carbonation chamber (Liang et al., 2019; Li et al., 2020). Stainless steel baskets with multiholes of less than 2 mm aperture size were customized and adopted to hold the samples of RCAs with various particle diameters in the carbonation chamber, as demonstrated in Supplementary Figure 3B, which ensured better all-round contact between the samples of RCA and CO₂ gas during the ACE of the RCA.

The ACE for the RCA samples was performed in this paper, and the corresponding detailed procedures for the ACE were described by Yang et al. (2023). The standard for the end of ACE for the RCA samples was that when the weight of the samples remained basically unchanged, the accelerated carbonation durations for this paper's experiment were all more than 160 min.

The apparent density (ρ_{app}) and water absorption (W_a) of the RCAs before and after ACE were measured based on the Chinese standard GB/T 14685-2022, 2022 to explore the degree to which the CRCA enhanced the properties, and the specific testing procedures and computational formulas used were described by Wu et al. (2023); Yang et al. (2023), and Ju et al. (2024). Notably, the whole CRCA samples with different particle diameters obtained by RCA after carbonation were put into an oven at a temperature of 105 ± 5°C to dry until a constant weight was reached. Subsequently, three parallel samples were used for testing the ρ_{app} and W_a of the CRCA (see Figure 4B, and the final ρ_{app} and W_a of the CRCA were the average values based on the three parallel samples.

Moreover, during our following investigations, both the apparent density (ρ_{app}) and water absorption (W_a) of the RCAs

before and after ACE were treated as the indexes for comparing and quantifying the properties enhancement degrees of NCA, RCA and CRCA, but the ITZ of RCA after the ACE test was not characterized in this paper.

2.2.2 Concrete mix proportions and specimen preparation

2.2.2.1 Mix proportions for the fresh concrete cast by NCA, RCA, and CRCA

Concrete specimens, i.e., NCAC, RCAC, and CRCAC, with their different coarse aggregate types, including NCA, RCA and CRCA, were prepared in accordance with the mix proportions in Table 2 (JGJ 55-2011, 2011). The coarse aggregates used for continuous grading and nominal diameters ranged from 5-10 mm, 10-20 mm, and 20-25 mm, and the particle grading distributions of the coarse aggregates in the concrete specimens, including the NCAC, RCAC, and CRCAC, are shown in Supplementary Figure 1A. Moreover, the other raw materials, including the cement, water, and fine aggregates (the particle grading distribution is shown in Supplementary Figure 1B, were consistent with those described in Section 2.1. In addition, the substitution rates of RCA and CRCA for preparing the RCAC and CRCAC based on Table 2 were both 100%.

2.2.2.2 Preparation of fresh concrete specimens

To minimize the adverse impacts of RCA and CRCA with high water absorption (Quattrone et al., 2016) on the workability, mechanical properties and durability of fresh RCAC and CRCAC, the RCA and CRCA were presaturated and drained one day before casting the RCAC and CRCAC specimens to ensure that the effective mix proportions of RCAC and CRCAC were consistent with those of NCAC (Xuan et al., 2016b). It was unnecessary to conduct the presaturation treatment for NCA due to its extremely low water absorption.

Sufficient experimental specimens of NCAC, RCAC and CRCAC with 100×100×100 mm³ cubes were cast and prepared according to the Chinese standard (JGJ 55-2011, 2011); these specimens were used to test the compressive strengths of NCAC, RCAC and CRCAC and to further explore the chloride transport characteristics and durability life of marine RC structures constructed from NCA, RCA and CRCA exposed to an artificial simulated marine environment of alternating drying-wetting cycles.

A total of 9 cubic specimens of 100×100×100 mm³ were utilized to determine the compressive strength of the concrete, and the number of each concrete type (NCAC, RCAC and CRCAC) included 3 parallel samples. The compressive strengths of the NCAC, RCAC and CRCAC specimens after 28 d of complete curing were measured by using a concrete pressure testing

TABLE 2 Mix proportions of fresh concrete with NCA, RCA and CRCA.

w/c	Cement (kg/m ³)	Water (kg/m ³)	Fine aggregate (kg/m ³)	Coarse aggregate (kg/m ³)
0.4	488	195	584	1134

machine, as shown in [Supplementary Figure 4](#). Moreover, 15 concrete cube specimens remained in total, and each concrete type (NCAC, RCAC and CRCAC) included 5 samples. After 28 d of curing ([He et al., 2023](#)), each specimen was thoroughly washed and dried under natural conditions. Two symmetrical surfaces of every concrete cube were reserved for chloride ion invasion, and the remaining 4 surfaces were sealed using an epoxy polyurethane-based coating, as shown in [Supplementary Figure 5](#).

2.2.3 Experiment of chloride transport in concrete specimens

2.2.3.1 Simulation of a marine drying-wetting alternating environment

Previous efforts have indicated that an alternating drying-wetting marine environment, i.e., the marine tidal zone and splash zone, has the greatest impact on the deterioration of durability of coastal RC structures ([Othmen et al., 2018](#); [Ju et al., 2021](#); [Fu et al., 2022](#); [Ju et al., 2022](#); [Wu et al., 2022](#); [Xia et al., 2023](#)). For our study, an indoor test of natural chloride transport in the concrete specimens of the NCAC, RCAC, and CRCAC under a simulated drying-wetting alternating marine environment was carried out to explore the effects of the NCA, RCA, and CRCA on the chloride profiles and chloride transport characteristics of various types of concrete. An automatic device for simulating the drying-wetting alternating marine environment independently developed by our scientific research team was used to achieve a marine tidal alternation of drying-wetting cycles based on a dry-wet ratio of 1:1. This automatic device was composed of two test chambers and a timed water conveyance system, and the latter was composed of pumps, time-control switches, water pipes, etc., as shown in [Supplementary Figure 6](#).

According to the time-control switches of the timed water conveyance system, the open and close functions of the pumps were regularly controlled to automatically achieve alternating continuous 12 h complete immersion in man-made seawater and continuous 12 h complete dry exposure to the atmosphere for the NCAC, RCAC, and CRCAC specimens on the right side of the test chamber. During the simulated drying-wetting alternating process of the marine diurnal tides, the drying-wetting cycle period was equal to 24 h, and the dry-wet ratio was considered 1:1. A 3.5% NaCl solution was adopted as the artificial seawater for our chloride transport experiment, and the artificial seawater in the test chambers was required to be termly updated every 10 d to ensure the accuracy of the final results. Moreover, the two test chambers were both sealed to prevent the evaporation of chloride solution during the stages of complete immersion, but the test chamber on the right side of [Supplementary Figure 6](#) should be unsealed during the stages of complete dry exposures.

The final duration of chloride ion transport in the NCAC, RCAC and CRCAC specimens exposed to the simulated drying-wetting marine environment (t_e) was 180 d. When t_e reached 60, 90, 120, 150 and 180 d, the corresponding experimental specimens were removed from the test chambers; subsequently, the chloride

penetration depths and chloride concentrations from the concrete surface to the inside were measured, as described in the following paragraphs.

2.2.3.2 Measurements of chloride penetration depth

As shown in [Supplementary Figure 7A](#), one of the chloride invasion surfaces for the NCAC, RCAC and CRCAC specimens at different exposure times was first selected and drilled along the chloride transport direction perpendicular to the surface (see [Supplementary Figure 7E](#)). At least 3 holes were drilled for each surface of the specimen, and the diameter and drilled depth of each arbitrary hole were at least 5 mm and 20 mm, respectively. Subsequently, the residual powders in the drilled holes were removed, a 0.1 mol/L AgNO₃ solution was titrated into the hole wall, and then, the colour reaction took approximately 10 min. Finally, the chloride penetration depths were measured based on the colour reaction depths in each drilled hole, and the final tested results were the average values of at least 3 drilled holes, as shown in [Supplementary Figure 7F](#). Note that the chloride penetration depth for each drilled hole needed to be tested at least 5 times, and the final results of the chloride penetration depth for concrete used the multimeasured average values of the entire drilled hole. The measurements of chloride penetration depth for concrete samples can be used to roughly/qualitatively analyse and compare the resistance to chloride penetration of NCAC, RCAC, and CRCAC.

2.2.3.3 Measurements of chloride concentration

As shown in [Supplementary Figure 7A](#), two chloride invasion surfaces, including the drilled and other symmetrical surfaces, of the NCAC, RCAC, and CRCAC specimens at different exposure times were selected, and a cement-based composite grinder was used to mill the concrete powders layer by layer beginning from the two surfaces of the concrete specimens to their inside along the chloride transport depth direction, as shown in [Supplementary Figure 7B](#). The thickness ground off for each layer within the concrete specimens was controlled at 2 mm from chloride transport depths of $x=0$ mm to $x=20$ mm. Subsequently, the various layers of the concrete powders were collected and placed in clean plastic sealing bags, as shown in [Supplementary Figure 7C](#). Finally, the water-soluble chloride concentrations within the NCAC, RCAC, and CRCAC powders were determined by using a rapid chloride ion content test device according to the Chinese standard ([JTJ 270-1998, 1998](#)), as shown in [Supplementary Figure 7D](#). Hence, for this paper's test, the chloride concentration within each concrete specimen at different exposure times is equivalent to the average value of two parallel samples. The measurements of chloride concentration for concrete samples can be used to reflect the variation trend of chloride concentrations vs. depth and to precisely/quantitatively represent the chloride profiles and transport characteristics of the NCAC, RCAC, and CRCAC.

Note: the tested free chloride concentrations in our study were all referred to as the percentage of the concrete mass (%).

3 Results and analysis

3.1 Comparison of the properties of NCA, RCA and CRCA

According to Section 2.2.1, the apparent density and water absorption results for the NCA, the RCA, and the CRCA with different particle diameters are presented in the Figures 2 and 3. The apparent density and water absorption of the CRCA were both between those of the NCA and RCA. Through analysis, the apparent density and water absorption for CRCA with different particle diameters are approximately 1.40-3.97% higher and approximately 16.3-21.8% lower than those of RCA, which indicates that the accelerated carbonation method based on gaseous CO₂ can effectively enhance the macroproperties of RCA.

3.2 Compressive strength of various concrete specimens

The measured compressive strength results for the NCAC, RCAC, and CRCAC specimens prepared by NCA, RCA and CRCA with continuous grading based on Section 2.2.2 were determined and are shown in Figure 11; the substitution rates of RCA and CRCA within the RCAC and CRCAC specimens are 100%.

From Figure 4, the average compressive strength of the CRCAC was 52.47 MPa, which is between those of the NCAC (54.37 MPa) and RCAC (47.43 MPa). The strength of concrete materials with different aggregate types strongly depends on the mechanical properties of the internal aggregates and cement pastes (Ge et al., 2021). Compared to those of NCA and CRCA, the material defects of RCA, including porosity and microcracks, result in the looseness and nonuniformity of the RCA and its RCAC, further affecting the overall strength and stability of the RCAC (Bao et al., 2023).

Moreover, the old and new interfacial transition zone (ITZ) as well as the incomplete hydration of cement particles can affect the strength of RCAC; in particular, the looser meso-scopic structure of the new ITZ for RCAC leads to a reduction in interfacial bonding performance, further decreasing the overall strength of RCAC (Patil et al., 2021), which is the reason for the decrease in strength of RCAC.

Additionally, the measured compressive strength of the CRCAC was only approximately 3.49% lower than that of the NCAC based on Figure 4. The results further demonstrate that the difference in the mechanical properties between the CRCAC and NCAC can be reduced by the accelerated carbonation modification method, and this good approach can provide some feasible, stable and reliable support for the promotion and application of the CRCAC and its CRCAC in marine infrastructures.

3.3 Chloride transport characteristics of marine RC structures

3.3.1 Chloride penetration depth

Figure 5 shows that the chloride penetration depths in the NCAC, RCAC and CRCAC gradually increase with increasing exposure time t_e . At an identical exposure time, the tested chloride penetration depth in NCAC is the smallest, that in RCAC is the largest, and that of CRCAC is between those of NCAC and RCAC. This result indicates that CRCA can increase the resistance of CRCAC to chloride penetration to a certain degree in an alternating drying-wetting marine environment and hence can effectively enhance the chloride ion penetration resistance of marine RC structures. This effect may be attributed to the densification degrees of internal pores and microcracks in the CRCA is greater than that in the RCA, which effectively blocks chloride penetration in the CRCA and CRCAC used for constructing marine infrastructures (Li et al., 2020).

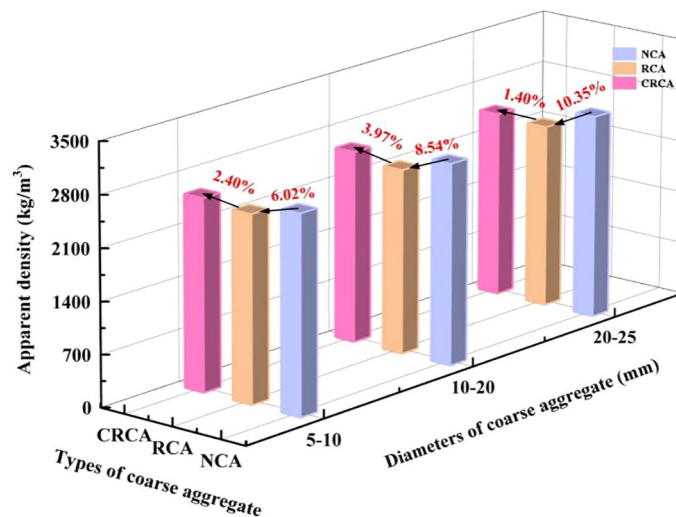


FIGURE 2 Apparent densities of coarse aggregates of various types and with various particle diameters.

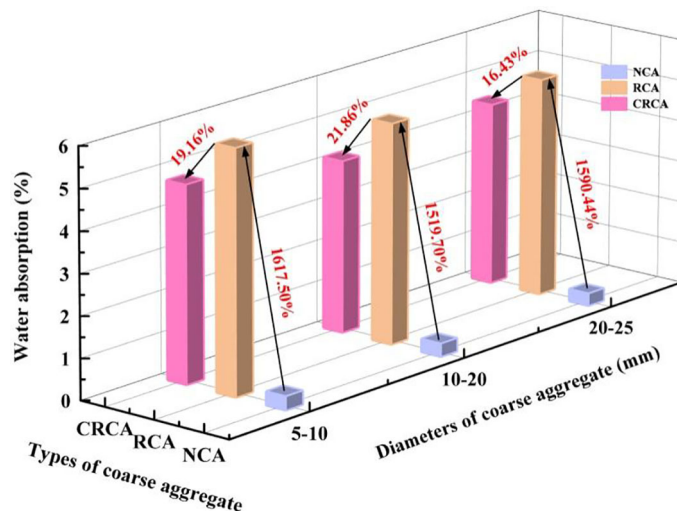


FIGURE 3 Water absorption of coarse aggregates of various types and with various particle diameters.

On the basis of Figure 13, we can observe that the chloride penetration depths in RCAC are approximately 1.04-1.18 times greater than those in CRCAC, i.e., the chloride penetration depth in CRCAC accounts for approximately 84.7-96.2% of that in RCAC, which demonstrates that using CRCA can effectively improve the resistance of RCAC to chloride penetration. Moreover, the tested chloride penetration depths of the NCAC were still lower than those of the CRCAC, and the resistance to chloride penetration of the CRCAC exhibited a difference of approximately 11.4-30.2% compared with that of the NCAC.

The chloride penetration depth results are shown in Figures 5 and 6, which can only be used to roughly and qualitatively analyse the effect of NCA, RCA, and CRCA on the resistance to chloride penetration of their corresponding concrete materials. The chloride profiles and transport characteristics of the NCAC, RCAC, and CRCAC used for marine infrastructures under alternating drying-

wetting marine environments still need to be accurately quantified and explored.

3.3.2 Chloride profiles

The alternating drying-wetting marine zone is the area where the RC structure is most seriously eroded by chloride ions (Nukushina, et al., 2021; Cao, et al., 2022), and the deterioration degree of RC structures exposed to alternating drying-wetting environments is greater than that in the underwater full immersion area, where chloride ions are transmitted by a pure diffusion mechanism (Sun et al., 2018). By means of Section 2.2.3, the chloride concentration profiles of the NCAC, RCAC, and CRCAC at various exposure periods are acquired, as plotted and exhibited in Figure 7. Clearly, the tested chloride concentrations of the NCAC, RCAC, and CRCAC gradually increasing as the depth

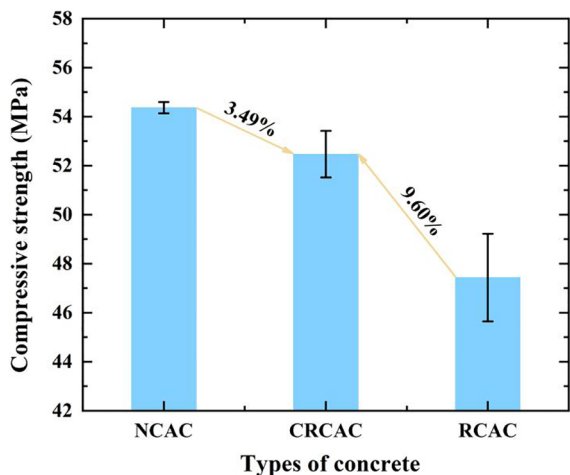


FIGURE 4 Compressive strength of the NCAC, CRCAC and RCAC specimens.

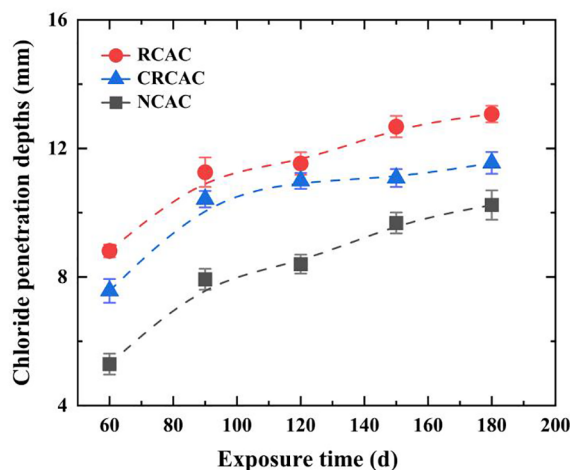


FIGURE 5 Time-dependent chloride penetration depths of the NCAC, CRCAC and RCAC specimens.

increases within the range of the convective zone (nearly 5 mm from the surface to the inside, along the chloride transport direction), and the skin effect of chloride ingress in concrete can be significantly observed (Andrade et al., 1997; Cai et al., 2020). The chloride concentrations of the different concrete types gradually decrease with increasing depth but increase with increasing exposure period in the stable diffusion zone (with depths greater than 5 mm). Due to the influence of the long-term drying–wetting alternating action of seawater, chloride ions are transported by the common mechanisms of “convection-diffusion” (Liu et al., 2021; Liu et al., 2022), resulting in an increase in the chloride concentrations within the concrete as the depth of the “first increase and then decrease” distribution characteristics increases (Kumar et al., 2021) and in the concrete near the surface area with the formation of a chloride concentration peak (Luo et al., 2021).

Figure 8 quantifies the relationship of chloride concentrations within the stable diffusion zones of NCAC, RCAC and CRCAC; the chloride concentrations in NCAC are the lowest, but those in RCAC are the largest, and those of CRCAC are between those of NCAC and RCAC, which are consistent with the results of the chloride penetration depth shown in Figures 5 and 6. The measured chloride concentrations in the RCAC are approximately 1.2–1.9 times those in the CRCAC, i.e., the chloride concentrations in the CRCAC account for approximately 52.6–83.3% of those in the RCAC. Although the chloride concentrations in the CRCAC are approximately 27–50% less than those in the NCAC, the chloride concentrations in the CRCAC are also significantly lower than those in the RCAC. The results indicate that the use of the CO₂ accelerated carbonation method for RCAs can effectively promote the densification of internal pores in CRCA and CRCAC and further intercept the passageway of microcracks within marine RC structures (Liang et al., 2019; Li et al., 2020); hence, long-term chloride transport concentrations are reduced, and finally, the durability of marine infrastructures exposed to salt environments is prolonged.

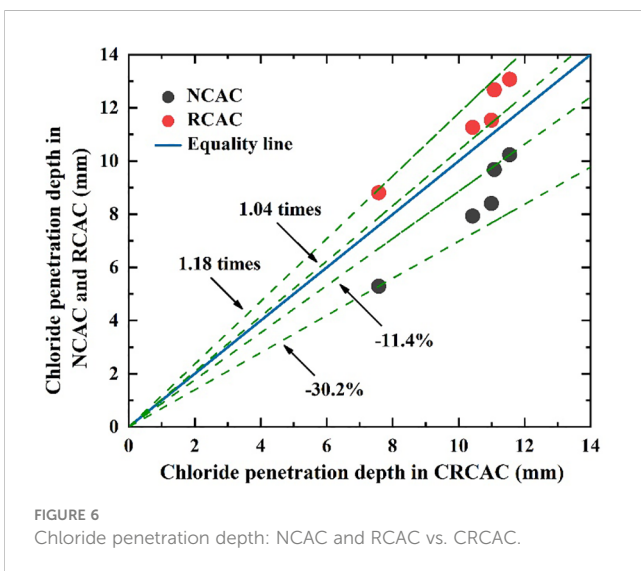


FIGURE 6 Chloride penetration depth: NCAC and RCAC vs. CRCAC.

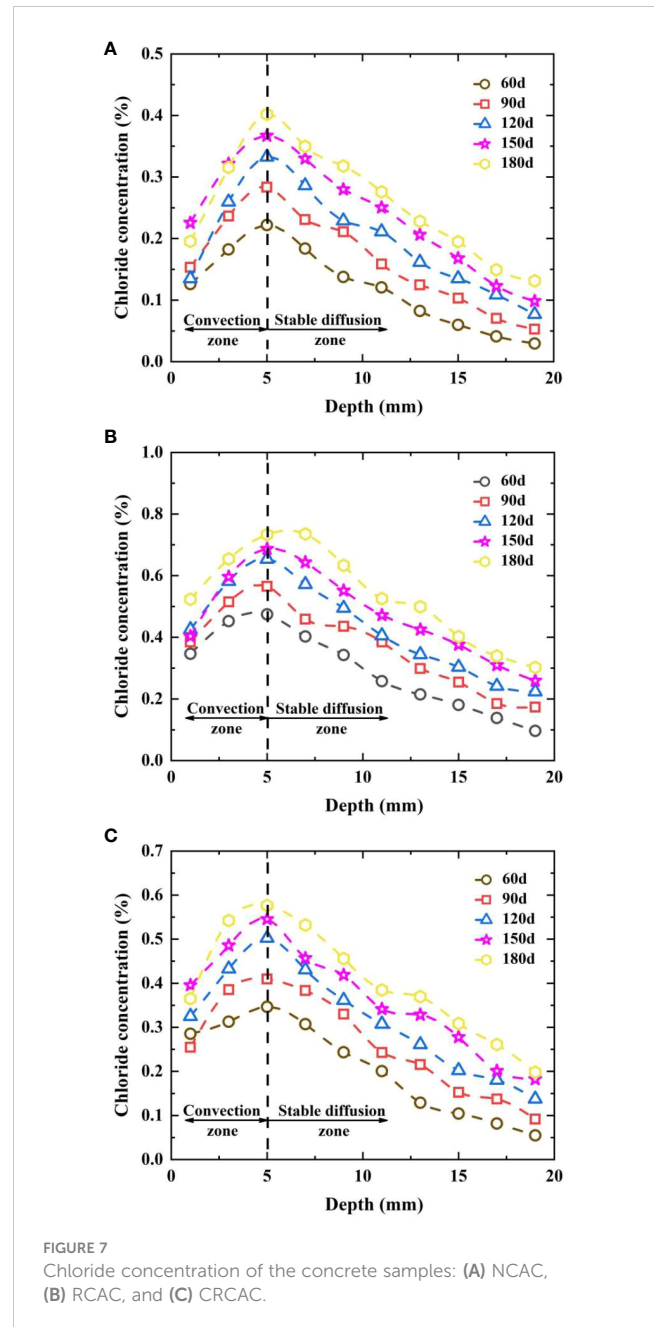


FIGURE 7 Chloride concentration of the concrete samples: (A) NCAC, (B) RCAC, and (C) CRCAC.

3.4 Modelling of chloride transport in marine RC structures

3.4.1 Fick’s second law of diffusion

The chloride profiles in the stable diffusion zone for the NCAC, RCAC, and CRCAC specimens are shown in Figure 14 can be quantified using Fick’s second law. Several significant parameters, including the surface chloride concentration (SCC), chloride diffusion coefficient (CDC), and ageing factor (AF) of concrete specimens with various coarse aggregate types, are determined via nonlinear regression analysis. These parameters were subsequently used to thoroughly analyse the effect of CRCA on the chloride transport characteristics of the CRCAC. The analytical solution expression of

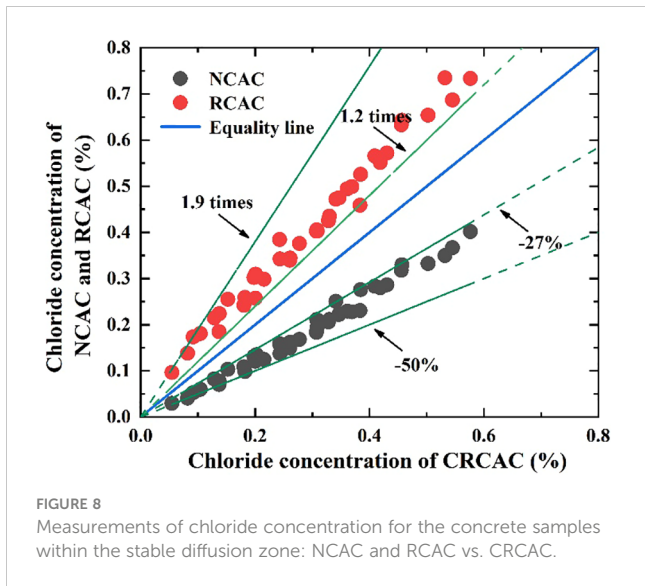


FIGURE 8 Measurements of chloride concentration for the concrete samples within the stable diffusion zone: NCAC and RCAC vs. CRCAC.

Fick's second law considering one-dimensional chloride diffusion in marine RC structures is expressed as (Othmen et al., 2018):

$$C(x, t) = C_s(t) \cdot \left[1 - \operatorname{erf} \left(\frac{x}{2\sqrt{D_{\text{app}}(t) \cdot t}} \right) \right] \quad (1)$$

$$D_{\text{app}}(t) = \frac{D_{\text{ref}}}{1-a} \left(\frac{t_{\text{ref}}}{t} \right)^a \quad (2)$$

where $C(x, t)$ is the free chloride concentration at different depths x and an arbitrary exposure time t_e (%); $C_s(t)$ denotes the time dependency of SCC for concrete materials (%); $D_{\text{app}}(t)$ is the time dependency of the apparent chloride diffusion coefficient (ACDC) of concrete materials (m^2/s), and its expression is shown in Equation (2) (Gašpárek et al., 2023); $\operatorname{erf}(\cdot)$ is the Gauss error function; D_{ref} is the reference chloride diffusion coefficient (RCDC) of concrete materials (m^2/s); a is the AF; moreover, t_{ref} is the reference exposure time, and $t_{\text{ref}} = 28$ d (Pontes et al., 2023).

3.4.2 Determination of $C_s(t)$, $D_{\text{app}}(t)$, D_{ref} , and a

The SCC, i.e., C_s , and the ACDC, i.e., D_{app} , for concrete specimens with various coarse aggregate types (NCA, RCA, and CRCA) and at different exposure periods t_e can be determined by fitting Equation (1) to the chloride profiles of the NCAC, RCAC, and CRCAC specimens in the ranges of the stable diffusion zone using the nonlinear regression method, as shown in Figure 9. The chloride measurements corresponding to the exposure times of $t_e=60, 90, 120,$ and 180 d are the original scatters for acquiring the results of C_s and D_{app} via regression analysis, as exhibited in Table 3.

Moreover, the tested chloride concentration values for an exposure period t_e of 150 d are used to verify the accuracy of the chloride transport model of marine RC structures with various coarse aggregate types, as detailed in the following sections.

The variations in the SCC, i.e., C_s , with increasing exposure period t_e for the NCAC, RCAC, and CRCAC specimens under the alternating drying-wetting marine environment are shown in Figure 10. The C_s values for the concrete specimens with different

coarse aggregate types exhibit a nonlinear increasing trend with increasing exposure time t_e , which is consistent with the findings reported in the existing published literature (Cai et al., 2021; Ortolan et al., 2023). Among them, the C_s values for NCAC are the lowest, but those for RCAC are the highest, and the C_s values of CRCAC are between those of NCAC and RCAC, which are consistent with the variation patterns of the chloride penetration depth and chloride concentrations shown in Figures 5–8.

$$C_s(t) = A \cdot \ln(t) + B \quad (3)$$

where A and B are the undetermined coefficients within $C_s(t)$ for the NCAC, RCAC, and CRCAC.

The coarse aggregate type coefficient, i.e., T_{ca} , is proposed to quantify the effects of NCA, RCA, and CRCA on the chloride

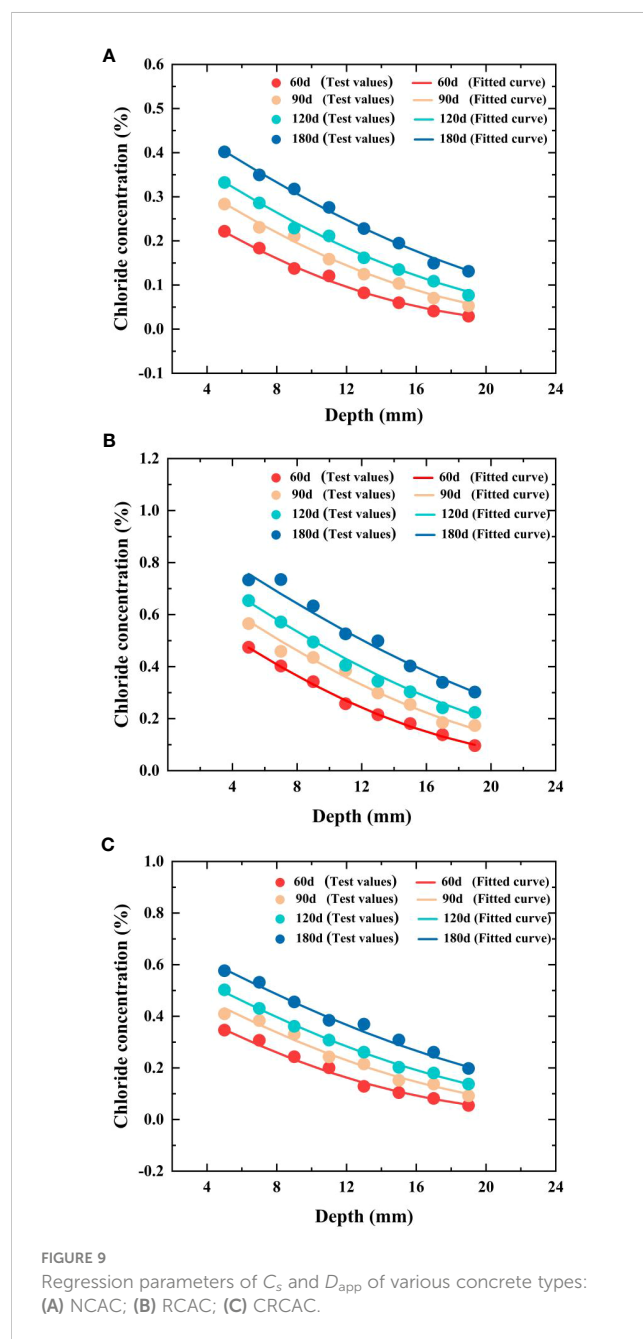


FIGURE 9 Regression parameters of C_s and D_{app} of various concrete types: (A) NCAC; (B) RCAC; (C) CRCAC.

TABLE 3 Regression parameters of C_s and D_{app} for NCAC, RCAC, and CRCAC.

t_e (d)	NCAC		RCAC		CRCAC	
	C_s (%)	D_{app} ($\times 10^{-12}$ m ² /s)	C_s (%)	D_{app} ($\times 10^{-12}$ m ² /s)	C_s (%)	D_{app} ($\times 10^{-12}$ m ² /s)
60	0.34	12.0	0.75	15.7	0.52	13.7
90	0.41	15.0	0.67	16.8	0.61	12.0
120	0.46	9.71	0.86	12.3	0.67	10.9
180	0.53	8.67	0.98	11.2	0.76	9.50

transport characteristics of marine RC structures with different coarse aggregate types. T_{ca} values of 0, 1, and 2 represent NCA and its NCAC, CRCA and its CRCAC, as well as RCA and its RCAC, respectively. On this basis, the relationships between the regression parameters A and B of the NCAC, RCAC and CRCAC specimens and T_{ca} are quantified within Equation (3), as shown in Figure 11. Parameter A shows a nearly linear growth trend with T_{ca} , and a linear function is adopted to fit, regress and determine the functional expression of $A(T_{ca})$, as shown in Figure 11. Moreover, parameter B is almost independent of T_{ca} . Therefore, the average value of B is -0.38207 , and this value is considered the final result for parameter B .

In summary, an empirical function for the time dependency of the SCC, i.e., $C_s(t)$, of concrete considering the coarse aggregate types (NCA, RCA, and CRCA) under alternating marine drying-wetting cycles is expressed as follows:

$$\begin{cases} C_s(T_{ca}, t) = A(T_{ca}) \cdot \ln(t) + B \\ A(T_{ca}) = 0.1758 + 0.042 \cdot T_{ca}, B = -0.3821 \end{cases} \quad (4)$$

The variations in the ACDC, i.e., D_{app} , with increasing exposure period for the NCAC, RCAC, and CRCAC specimens under the alternating drying-wetting marine environment are shown in Figure 12. The D_{app} values for marine RC structures with different coarse aggregate types show a nonlinear decreasing trend with increasing exposure time t_e , which is consistent with the results

reported in the literature (Titi and Tabatabai, 2018; Zhang et al., 2020, 2022; Vintimilla et al., 2023). Among them, the D_{app} values of NCAC are the lowest, but those of RCAC are the highest, and the D_{app} values of CRCAC are between those of NCAC and RCAC, which are consistent with the variation patterns of chloride penetration depth, chloride concentrations and SCCs in the previous sections of this paper. Therefore, CRCA can effectively densify the internal pores and microcracks within CRCAC (Liang et al., 2019; Li et al., 2020), consequently decreasing the ACDC, i.e., the velocity of chloride transport into concrete, of CRCAC and reducing the chloride concentration in marine RC structures.

The time dependency of the power function form [shown in Equation (2)] is utilized to establish the relationship between D_{app} scatters and the exposure period t_e for the NCAC, RCAC, and CRCAC specimens to determine the RCDC, i.e., D_{ref} , and the AF, i.e., a . The fitted curves are shown in Figure 12, and the regression results are exhibited in Table 4. On the basis of this figure and table, we can clearly observe that the magnitude and variation trend of D_{ref} with different coarse aggregate types are in agreement with those of D_{app} ; specifically, the D_{ref} values of CRCAC are between those of NCAC and RCAC.

The impact factor of the coarse aggregate type, i.e., $f_{ca}(T_{ca})$, is defined to quantify the influence of different coarse aggregate types on the chloride diffusion coefficient of marine RC structures, expressed as follows:

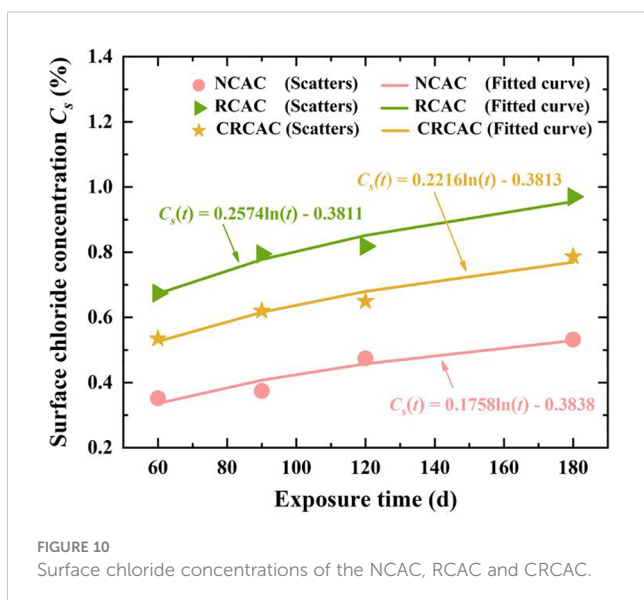


FIGURE 10 Surface chloride concentrations of the NCAC, RCAC and CRCAC.

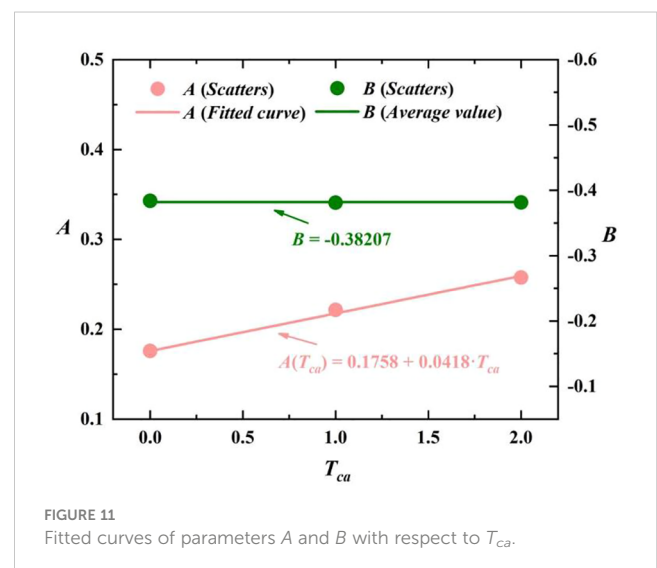


FIGURE 11 Fitted curves of parameters A and B with respect to T_{ca} .

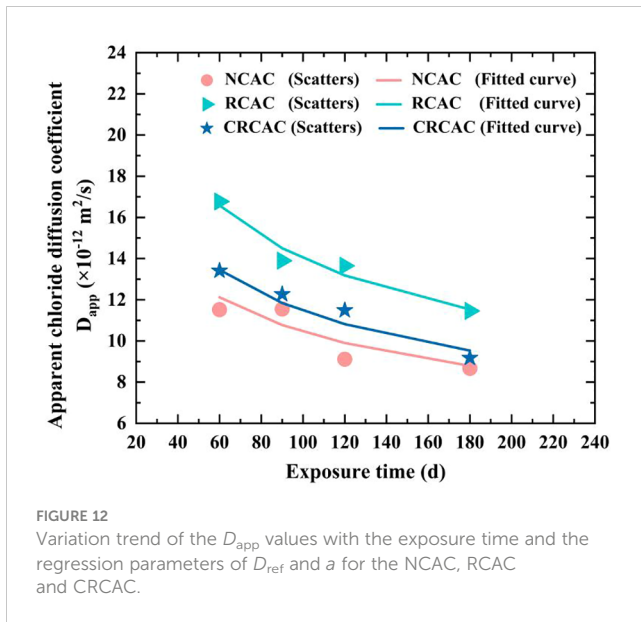


FIGURE 12 Variation trend of the D_{app} values with the exposure time and the regression parameters of D_{ref} and a for the NCAC, RCAC and CRCAC.

$$f(T_{ca}) = D_{ref}(T_{ca})/D_{ref}(0) \tag{5}$$

where $D_{ref}(T_{ca})$ is the RCDC of marine RC structures with different coarse aggregate types (m^2/s) and $D_{ref}(0)$ is the RCDC of the NCAC (m^2/s). On the basis of Table 4, $D_{ref}(0)=D_{ref}(T_{ca}=0)=10.72 \times 10^{-12} m^2/s$, $D_{ref}(T_{ca}=1)=11.72 \times 10^{-12} m^2/s$, and $D_{ref}(T_{ca}=2)=14.27 \times 10^{-12} m^2/s$.

The results of the impact factor $f_{ca}(T_{ca})$ for the NCAC, RCAC and CRCAC specimens are confirmed in accordance with these D_{ref} values and Equation (5), and the variations in f_{ca} scatter with T_{ca} are plotted in Figure 13. From this figure, f_{ca} shows a nonlinear increasing trend with the variation in T_{ca} , and the empirical function of $f_{ca}(T_{ca})$ is fitted and determined by using nonlinear regression analysis. In addition, evident linear variation trends between the AFs a and T_{ca} are observed, and a linear functional expression of $a(T_{ca})$ is acquired in Figure 13.

In summary, an empirical expression for the time dependency of the ACDC, i.e., $D_{app}(t)$, of the marine RC structure accounting for coarse aggregate types (NCA, RCA and CRCA) under alternating marine drying-wetting cycles is determined as follows:

$$\begin{cases} D_{app}(T_{ca}, t) = \frac{D_{ref}(T_{ca})}{1-a(T_{ca})} \left(\frac{t_{ref}}{t}\right)^{a(T_{ca})} \\ D_{ref}(T_{ca}) = D_{ref}(0) \cdot f_{ca}(T_{ca}) \\ f_{ca}(T_{ca}) = 1 + 0.021 \cdot T_{ca} + 0.0723 \cdot T_{ca}^2 \\ a(T_{ca}) = 0.2922 + 0.01977 \cdot T_{ca} \end{cases} \tag{6}$$

TABLE 4 Regression parameters of D_{ref} and a for NCAC, RCAC, and CRCAC.

Concrete type	NCAC	RCAC	CRCAC
$D_{ref} (\times 10^{-12} m^2/s)$	10.72	11.72	14.27
a	0.29	0.32	0.33

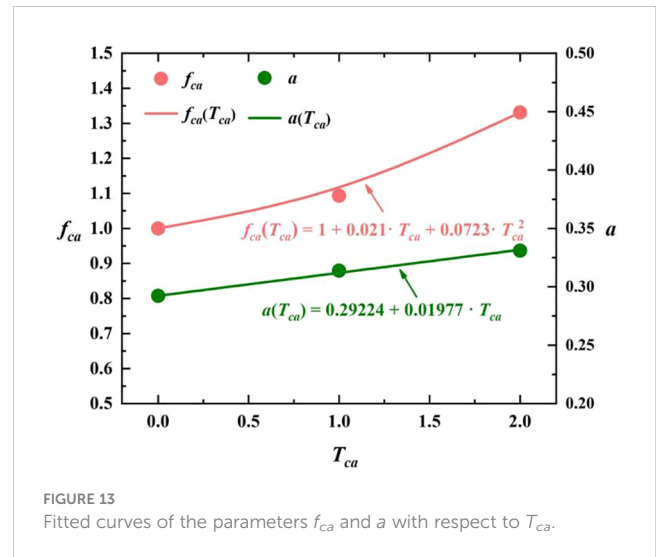


FIGURE 13 Fitted curves of the parameters f_{ca} and a with respect to T_{ca} .

3.4.3 Establishment of a chloride transport model for marine RC structures

A computational model of chloride transport in marine RC structures considering coarse aggregate types (NCA, RCA, and CRCA) is established by combining Equations (1), (2), (4), and (6). The effects of the coarse aggregate type on the time dependency of SCC $[C_s(t)]$ and the ACDC $[D_{app}(t)]$ are both simultaneously considered in this proposed model, as expressed:

$$\begin{cases} C(x, T_{ca}, t) = C_s(T_{ca}, t) \left[1 - \operatorname{erf} \left(\frac{x}{2\sqrt{D_{app}(T_{ca}, t)}} \right) \right] \\ D_{app}(T_{ca}, t) = \frac{D_{ref}(T_{ca})}{1-a(T_{ca})} \left(\frac{t_{ref}}{t}\right)^{a(T_{ca})} \\ C_s(T_{ca}, t) = A(T_{ca}) \cdot \ln(t) + B \\ A(T_{ca}) = 0.1758 + 0.042 \cdot T_{ca}, B = -0.3821 \\ D_{ref}(T_{ca}) = D_{ref}(0) \cdot f_{ca}(T_{ca}) \\ f_{ca}(T_{ca}) = 1 + 0.021 \cdot T_{ca} + 0.0723 \cdot T_{ca}^2 \\ D_{ref}(0) = 1.072 \times 10^{-11} m^2/s \\ a(T_{ca}) = 0.2922 + 0.01977 \cdot T_{ca} \end{cases} \tag{7}$$

This chloride transport model [Equation (7)] can be applied to assess and predict the chloride profiles for marine RC structures with various coarse aggregate types of NCA, RCA, and CRCA at arbitrary exposure times t_e under the precondition of $w/c=0.4$. In particular, when $T_{ca}=1$, this computational model can be utilized to analyse and evaluate the long-term chloride transport behaviours of marine RC structures constructed by using the CRCAC under an alternating marine drying-wetting environment, which can provide a vital theoretical foundation for evaluating the durability life of marine RC structures cast by the CRCA.

3.4.4 Model verification

To verify the accuracy of this paper's proposed chloride transport model [Equation (7)], the tested chloride concentrations for the NCAC, RCAC and CRCAC at $t_e=150$ d (exhibited in Figure 7) were compared with those evaluated via Equation (7), as shown in Figure 14.

On the basis of this figure, the chloride concentrations acquired by the model of Equation (7) were in agreement with those from this paper’s experimental measurements. The chloride concentrations of the NCAC, RCAC and CRCAC samples predicted by our proposed model against the experimental results at $t_e=150$ d are shown in Figure 15. Based on Figure 15, almost all of the model results determined by Equation (7) and our experiments are included in a relative error margin of $\pm 15\%$ for the NCAC, RCAC, and CRCAC, validating the accuracy of the chloride transport model of marine RC structures.

4 Durability life evaluation for a certain harbour wharf

Taking the RC beam components within a certain harbour wharf exposed to a corrosive environment of marine tidal zone as an example, the durability life of the RC beams constructed by the NCAC, RCAC and CRCAC were evaluated based on this paper’s proposed chloride transport model [Equation (7)] of marine infrastructures and the time-dependent corrosion rate model of reinforcement. The concrete mix proportions of the RC beam are described in Table 2. The cover thickness of the RC beam is 60 mm in the tensile area, and the rebar diameter is 25 mm. The design strength of the concrete materials for the RC beam of the wharf is considered greater than that of C35 based on the Chinese standard JTJ 153-2015, 2015. In fact, the tested compressive strengths of the NCAC and CRCAC are greater than 50 MPa, and the measured compressive strength of the RCAC is 45 MPa greater, as shown in Figure 4. The geometric dimensions of the RC beam are shown in Figure 16.

According to the mechanism of chloride-induced steel corrosion and marine structural performance degradation, the service life of marine RC structures can be treated in four stages, including the initial corrosion time of the steel bar t_i , the concrete cover cracking time t_s , the time that affects the normal use of RC

structures t_z , and the time that affects the structural bearing capacity t_c (Xiaoping et al., 2016). Considering the safety reserve of marine RC structures during operation, the sum of the initial corrosion time of the steel bar and the concrete cover cracking time are used as the basis for evaluating the durability life of RC beams within the harbour wharf (Xu et al., 2019), i.e., $t_d=t_i+t_s$.

4.1 Initial corrosion time of steel bar, t_i

According to Cao et al. (2019), the chloride threshold value range for RC structures exposed to corrosive marine environments is approximately 0.97-2.3% (the percentage of the cementitious material mass) when $w/c=0.4$ (Song et al., 2007). Taking the average value, i.e., $C_{cr(ce)}=1.635\%$, as the basis, the chloride threshold value for marine RC structures considering $w/c=0.4$ is converted to the percentage of the concrete mass, i.e., $C_{cr(con)}=0.327\%$, based on the concrete mix proportions in Table 2.

By setting $C(x, T_{ca}, t)=C(c=60 \text{ mm}, T_{ca}, t_i)=0.327\%$ at the left side of Equation (7) and inserting the corresponding chloride transport parameters at the right side of Equation (7), the results of the initial corrosion time of steel bars for the RC beams cast by using the NCAC, RCAC, and CRCAC were evaluated based on this paper’s proposed chloride transport model of marine infrastructures, as shown in Table 5.

4.2 Concrete cover cracking time, t_s

According to the achievements reported by Ju et al. (2021), the concrete cover cracking time can be evaluated via the following equation:

$$t_s = \left\{ \frac{c \cdot [0.0228 \cdot \frac{c}{d} + 0.0016 \cdot f_{cuk} + 0.0343]}{(1 - w/c)^{-1.64}} \right\}^{1.4} \tag{8}$$

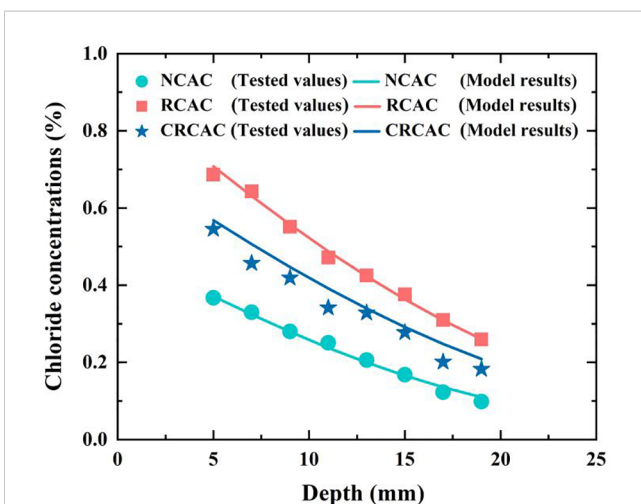


FIGURE 14 Comparison of chloride profiles determined by the model and experiments for the NCAC, RCAC, and CRCAC when the exposure time is 150 d.

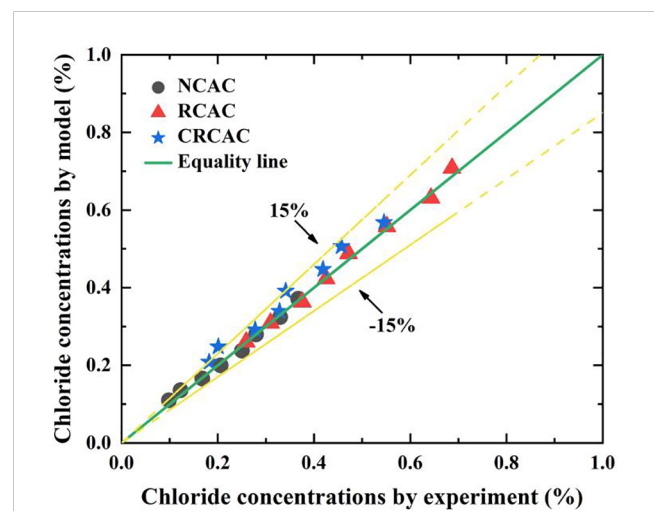


FIGURE 15 Comparison of chloride concentrations for the NCAC, RCAC and CRCAC evaluated by the model versus those of the experimental results.

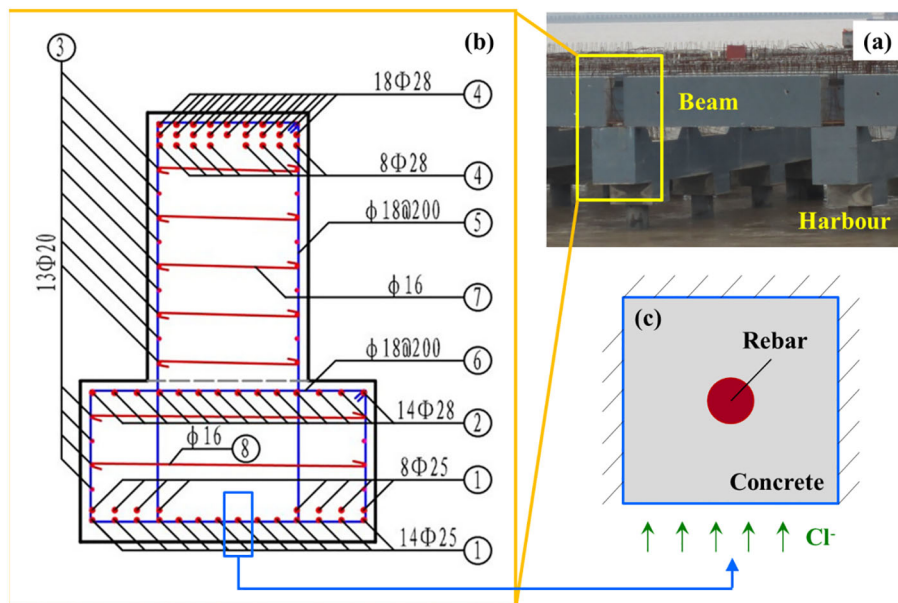


FIGURE 16 A certain harbour wharf: (A) real structure (under construction); (B) reinforcement drawing of an RC beam; (C) chloride transport in an RC beam.

where c denotes the cover thickness of the concrete, and $c=60$ mm; d is the diameter of the reinforcement, i.e., $d=25$ mm; and $f_{cu,k}$ is the standard compressive strength of the concrete, as shown in Figure 4; w/c is the water-cement ratio of the concrete materials, and $w/c=0.4$.

By substituting all the known parameters into Equation (8), the results of the concrete cover cracking time, t_s , for the RC beams within the harbour wharf constructed by NCA, RCA and CRCA are evaluated, as shown in Table 5.

4.3 Evaluation of the durability life of RC beams within harbour wharfs

Summarizing the evaluation results of the initial rebar corrosion time t_i in Table 5 and the concrete cover cracking time t_s in Table 5, the durability life results for the RC beam within the harbour wharf built by the NCAC, RCAC, and CRCAC, i.e., t_d , are determined and exhibited as follows:

The results indicated that the durability lifetimes of marine RC structures built with NCAC, RCAC, and CRCAC differ due to the various resistances to chloride ions. Among them, the durability life of the RC beam cast by the NCAC is the longest (almost $t_d=23$ a), but the durability life of the RC beam cast by the RCAC is the shortest ($t_d=13.82$ a), and the durability life of the RC beam constructed by the CRCAC ($t_d=17.7$ a) is between those of the NCAC and RCAC. Pang and Li (2016) derived probability models of chloride ingress parameters for predicting the service life of marine structures. The results indicated that the service life of OPC concrete structures is approximately 17-22.5 years when exposed to marine environments, validating the correctness and reasonability of this paper's evaluations.

In summary, based on the durability life results of marine structures, the durability of the marine RC infrastructures prepared

TABLE 5 Durability life of RC structure with NCAC, CRCAC and RCAC.

Types of concrete	NCAC	CRCAC	RCAC
t_i	15.80	10.72	7.300
t_s	7.160	6.980	6.520
t_d	22.96	17.70	13.82

by the CRCAC was approximately 28.10% greater than that of the RCAC. Although there are still differences compared with those of marine NCAC structures, the chloride penetration resistance and durability life of marine RC structures built via CRCAC are still improved to a certain extent compared with those of the RCAC, which can greatly promote the feasibility of using CRCAC in the construction, operation and maintenance of marine infrastructures.

5 Conclusions

In this paper, an indoor experiment for chloride transport in NCAC, RCAC, and CRCAC specimens under an artificial simulated marine environment with alternating drying-wetting cycles was conducted to examine the chloride profiles and transport characteristics of the NCAC, RCAC, and CRCAC concrete types, and a chloride transport model of marine RC structures considering coarse aggregate types in a marine tidal environment was established based on Fick's second law. Moreover, the durability life of marine RC beams within a certain harbour wharf constructed by the application of NCAC, RCAC, and CRCAC was evaluated and compared.

Some critical conclusions are listed as follows:

- (1) The apparent density and water absorption for CRCA with different particle diameters increased by approximately 1.40-3.97% and decreased by approximately 16.3-21.8% compared with those of the RCA, and the measured compressive strength for CRCAC was only approximately 3.49% lower than that of NCAC, indicating that the accelerated carbonation method based on gaseous CO₂ can effectively enhance the properties of RCA and reduce the difference in mechanical properties between CRCAC and NCAC.
- (2) The chloride penetration depths, chloride concentration profiles, surface chloride concentrations (SCCs), and chloride diffusion coefficients (CDCs) of the CRCAC are all between those of the NCAC and RCAC, which indicates that using the CRCA can effectively improve the resistance to chloride penetration and durability of marine RC structures exposed to marine tidal environments.
- (3) The SCCs and ACDCs for marine RC structures with NCA, RCA, and CRCA at various exposure periods are determined, and the effects of coarse aggregate type on the time dependency of SCC and ACDC are quantified. On the basis of the empirical expressions, a chloride transport model for marine RC structures considering coarse aggregate types is built, and the accuracy of this proposed model is verified.
- (4) Taking the RC beams within a certain harbour wharf as an example, the durability life results of the RC beams constructed by the NCAC, RCAC and CRCAC are evaluated based on this paper's proposed chloride transport model [Equation (7)] of marine infrastructures and the time-dependent corrosion rate model of reinforcement. The results showed that the durability life of the marine RC infrastructure prepared by the CRCAC was approximately 28.10% greater than that of the RCAC. Although there are still differences compared with those of marine NCAC structures, the chloride penetration resistance and durability life of marine RC structures built via CRCAC are still improved to a certain extent compared with those of the RCAC, which can greatly promote the feasibility of using CRCAC in the construction, operation and maintenance of marine infrastructures.

To sum up, our investigations can provide a scientific basis for the resource utilization of waste concrete, facilitate the practical application of RCAs and RCACs in marine infrastructures, and further help to improve the durability, reliability, stability and risk resistance of marine RC structures to support the design and construction of marine infrastructure, which has vital scientific significance, engineering value and development prospects.

For future studies, we will try our best to continuously carry out the relevant works and strive to be able to achieve the use of CRCA in the construction and operation of marine infrastructures to completely replace the NCA, as well as to ensure and even further

enhance the durability, reliability, stability and risk resistance of marine RC structures and provide support for the design and construction of marine infrastructures.

Data availability statement

The raw data supporting the conclusions of this article will be made available by the authors, without undue reservation.

Author contributions

HJ: Conceptualization, Methodology, Writing – original draft. LW: Investigation, Writing – original draft. XLJ: Formal analysis, Validation, Writing – original draft. ML: Writing – review & editing. ZX: Supervision, Writing – original draft. LG: Visualization, Writing – original draft. XHJ: Formal analysis, Validation, Writing – original draft. YL: Resources, Supervision, Writing – original draft. JL: Writing – review & editing.

Funding

The author(s) declare financial support was received for the research, authorship, and/or publication of this article. This research was supported by the National Key R&D Program of China (No: 2022YFB3207400), the Research and Innovation Program for Graduate Students in Chongqing (No: CYS23487), the National Natural Science Foundation of China (No: 52209156), and the 2023 National College Students' Innovation and Entrepreneurship Training Program (No. S202310618012).

Conflict of interest

Author LG was employed by the company Sichuan Communication Surveying & Design Institute Co. Ltd.

The remaining authors declare that the research was conducted in the absence of any commercial or financial relationships that could be construed as a potential conflict of interest.

Publisher's note

All claims expressed in this article are solely those of the authors and do not necessarily represent those of their affiliated organizations, or those of the publisher, the editors and the reviewers. Any product that may be evaluated in this article, or claim that may be made by its manufacturer, is not guaranteed or endorsed by the publisher.

Supplementary material

The Supplementary Material for this article can be found online at: <https://www.frontiersin.org/articles/10.3389/fmars.2024.1357186/full#supplementary-material>

References

- Andrade, C., Díez, J. M., and Alonso, C. (1997). Mathematical modeling of a concrete surface "Skin effect" on diffusion in chloride contaminated media. *Advanced Cement Based Materials* 6, 39–44. doi: 10.1016/S1065-7355(97)00002-3
- Ashrafian, A., Panahi, E., Salehi, S., and Amiri, M. J. T. (2022). On the implementation of the interpretable data-intelligence model for designing service life of structural concrete in a marine environment. *Ocean Eng.* 256. doi: 10.1016/j.oceaneng.2022.111523
- Bangley, C. W., Hasselman, D. J., Flemming, J. M., Whoriskey, F. G., Culina, J., Enders, L., et al. (2022). Modeling the probability of overlap between marine fish distributions and marine renewable energy infrastructure using acoustic telemetry data. *Front. Mar. Sci.* 9. doi: 10.3389/fmars.2022.851757
- Bao, J., Wei, J., Zhang, P., Zhuang, Z., and Zhao, T. (2022). Experimental and theoretical investigation of chloride ingress into concrete exposed to real marine environment. *Cement Concrete Composites* 130. doi: 10.1016/j.cemconcomp.2022.104511
- Bao, J., Zhang, H., Fang, X., Zhang, P., Qin, L., and Sun, J. (2023). Properties of recycled coarse aggregate concrete modified by silica nanoparticles: A short review. *J. Chin. Ceramic Soc.* 51, 2045–2053.
- Cai, R., Hu, Y., Yu, M., Liao, W., Yang, L., Kumar, A., et al. (2020). Skin effect of chloride ingress in marine concrete: A review on the convection zone. *Construction Building Materials* 262, 120566. doi: 10.1016/j.conbuildmat.2020.120566
- Cai, R., Yu, M., Hu, Y., Yang, L., and Ma, H. (2021). Influence of data acquisition and processing on surface chloride concentration of marine concrete. *Construction Building Materials* 273. doi: 10.1016/j.conbuildmat.2020.121705
- Cao, Y., Gehlen, C., Angst, U., Wang, L., Wang, Z. D., and Yao, Y. (2019). Critical chloride content in reinforced concrete - An updated review considering Chinese experience. *Cement Concrete Res.* 117, 58–68. doi: 10.1016/j.cemconres.2018.11.020
- Cao, J., Jin, Z., Ding, Q., Xiong, C., and Zhang, G. (2022). Influence of the dry/wet ratio on the chloride convection zone of concrete in a marine environment. *Construction Building Materials* 316. doi: 10.1016/j.conbuildmat.2021.125794
- Das, J. K., and Pradhan, B. (2023). Significance of chloride salt type and sulfate salt on chloride transport mechanism of concrete in the presence of corrosion inhibiting admixtures. *Construction Building Materials* 387. doi: 10.1016/j.conbuildmat.2023.131658
- de Vera, G., Antón, C., and Climent, M. A. (2024). Effect of exposure conditions on the chloride concentration profiles in a marine concrete structure, studied by means of the kernel density estimation technique and a Gaussian-Lorentzian model. *Construction Building Materials* 413. doi: 10.1016/j.conbuildmat.2023.134833
- Feng, C. H., Cui, B. W., Huang, Y. O. G., Guo, H., Zhang, W. Y., and Zhu, J. P. (2022). Enhancement technologies of recycled aggregate - Enhancement mechanism, influencing factors, improvement effects, technical difficulties, life cycle assessment. *Construction Building Materials* 317. doi: 10.1016/j.conbuildmat.2021.126168
- Fu, Q. L., Lian, F. Q., Liu, S. Y., Zhou, J. Y., Lu, L. L., Wang, J. F., et al. (2022). Seawater resistance mechanism of reinforcing bar-concrete composite structures restored by repair material incorporating multiple admixtures in a simulated marine splash zone. *Ocean Eng.* 253. doi: 10.1016/j.oceaneng.2022.111316
- Gao, Y. H., Zheng, Y. Y., Zhang, J. Z., Wang, J. D., Zhou, X. Y., and Zhang, Y. R. (2019). Randomness of critical chloride concentration of reinforcement corrosion in reinforced concrete flexural members in a tidal environment. *Ocean Eng.* 172, 330–341. doi: 10.1016/j.oceaneng.2018.11.038
- Gašpárek, J., Hůlek, L., Paulik, P., and Janotka, I. (2023). Theoretical prediction of chloride diffusion into concrete compared to natural chloride contamination of existing bridges. *Structures* 57. doi: 10.1016/j.istruc.2023.105080
- GB/T 14685-2022. (2022). Standard for Pebble and crushed stone for construction. (in Chinese).
- Ge, P., Huang, W., Quan, W., and Guo, Y. (2021). Research on compressive strength calculation of hybrid recycled aggregate concrete. *J. Huazhong Univ. Sci. Technology.* Nat. Sci. 49, 86–91.
- He, R., and Lu, N. (2023). Unveiling the dielectric property change of concrete during hardening process by ground penetrating radar with the antenna frequency of 1.6 GHz and 2.6 GHz. *Cement Concrete Composites* 144. doi: 10.1016/j.cemconcomp.2023.105279
- He, R., Nantung, T., Olek, J., and Lu, N. (2023). Field study of the dielectric constant of concrete: A parameter less sensitive to environmental variations than electrical resistivity. *J. Building Eng.* 74. doi: 10.1016/j.jobe.2023.106938
- Hosseini Zadeh, A., Mamirov, M., Kim, S., and Hu, J. (2021). CO₂-treatment of recycled concrete aggregates to improve mechanical and environmental properties for unbound applications. *Construction Building Materials* 275. doi: 10.1016/j.conbuildmat.2020.122180
- JGJ 55-2011. (2011). *Ordinary Concrete Mix Design Procedure* (Beijing, China: China Architecture & Building Press).
- JTJ 153-2015. (2015). *Standard for Durability Design of Port and Waterway Engineering Structure* (Beijing, China: China Communication Press).
- JTJ 270-1998. (1998). Standard for Testing code of concrete for port and waterway engineering. 67.
- Ju, X., Wu, L., Liu, M., Jiang, H., and Zhang, W. (2022). Modelling of chloride concentration profiles in concrete by the consideration of concrete material factors under marine tidal environment. *J. Mar. Sci. Eng.* 10. doi: 10.3390/jmse10070917
- Ju, X. L., Wu, L. J., Liu, M. W., Jiang, H., Zhang, W. X., Guan, L., et al. (2024). Influence of the original concrete strength and initial moisture condition on the properties improvement of recycled coarse aggregate via accelerated carbonation reactions. *Materials* 17. doi: 10.3390/ma17030706
- Ju, X., Wu, L., Liu, M., Zhang, H., and Li, T. (2021). Service life prediction for reinforced concrete wharf considering the influence of chloride erosion dimension. *Materials Rev.* 35, 24075.
- Korec, E., Jirásek, M., Wong, H. S., and Martínez-Pañeda, E. (2024). Phase-field chemo-mechanical modelling of corrosion-induced cracking in reinforced concrete subjected to non-uniform chloride-induced corrosion. *Theor. Appl. Fracture Mechanics* 129. doi: 10.1016/j.tafmec.2023.104233
- Kumar, S., Yang, E. H., and Unluer, C. (2021). Investigation of chloride penetration in carbonated reactive magnesia cement mixes exposed to cyclic wetting-drying. *Construction Building Materials* 284. doi: 10.1016/j.conbuildmat.2021.122837
- Lai, N., Li, L., Yang, C. Y., and Li, J. P. (2023). Service life of RC seawall under chloride invasion: A theoretical model incorporating convection-diffusion effect. *Ocean Eng.* 279. doi: 10.1016/j.oceaneng.2023.114590
- Li, Y., Fu, T., Wang, R., and Li, Y. (2020). An assessment of microcracks in the interfacial transition zone of recycled concrete aggregates cured by CO₂. *Construction Building Materials* 236. doi: 10.1016/j.conbuildmat.2019.117543
- Liang, C., Ma, H., Pan, Y., Ma, Z., Duan, Z., and He, Z. (2019). Chloride permeability and the caused steel corrosion in the concrete with carbonated recycled aggregate. *Construction Building Materials* 218, 506–518. doi: 10.1016/j.conbuildmat.2019.05.136
- Liang, C., Pan, B., Ma, Z., He, Z., and Duan, Z. (2020). Utilization of CO₂ curing to enhance the properties of recycled aggregate and prepared concrete: A review. *Cement Concrete Composites* 105. doi: 10.1016/j.cemconcomp.2019.103446
- Liu, H., and Jiang, L. (2021). Influence of Hydrostatic Pressure and Cationic Type on the Diffusion Behavior of Chloride in Concrete. *Materials* 14 (11). doi: 10.3390/ma14112851
- Liu, Q., Sun, L., Zhu, X., Xu, L., and Zhao, G. (2022). Chloride transport in the reinforced concrete column under the marine environment: Distinguish the atmospheric, tidal-splash and submerged zones. *Structures* 39, 365–377. doi: 10.1016/j.istruc.2022.03.041
- Luo, Y., Niu, D., and Su, L. (2021). Chloride Diffusion Property of Hybrid Basalt-Polypropylene Fibre-Reinforced Concrete in a Chloride-Sulphate Composite Environment under Drying-Wetting Cycles. *Materials (Basel)* 14 (5). doi: 10.3390/ma14051138
- Nukushina, T., Takahashi, Y., and Ishida, T. (2021). Numerical Simulations of Chloride Transport in Concrete Considering Connectivity of Chloride Migration Channels in Unsaturated Pores. *J. Advanced Concrete Technol.* 19 (7), 847–863. doi: 10.3151/jact.19.847
- Ortolan, T. L. P., Borges, P. M., Silvestro, L., da Silva, S. R., Possan, E., and Andrade, J. (2023). Durability of concrete incorporating recycled coarse aggregates: carbonation and service life prediction under chloride-induced corrosion. *Construction Building Materials* 404. doi: 10.1016/j.conbuildmat.2023.133267
- Othmen, I., Bonnet, S., and Schoefs, F. (2018). Statistical investigation of different analysis methods for chloride profiles within a real structure in a marine environment. *Ocean Eng.* 157, 96–107. doi: 10.1016/j.oceaneng.2018.03.040
- Ou, Y., Xu, M., Chen, D., Jiang, M., Xiao, L., and Mei, G. (2022). Effect of reverse water pressure on chloride penetration within finite concrete during drying-wetting cycles. *Ocean Eng.* 257, 111606. doi: 10.1016/j.oceaneng.2022.111606
- Pandey, S., and Rajhans, P. (2023). Durability assessment of quaternary blended recycled aggregate concrete under chloride environment. *Materials Today: Proc.* doi: 10.1016/j.matpr.2023.03.686
- Pang, L., and Li, Q. W. (2016). Service life prediction of RC structures in marine environment using long term chloride ingress data: Comparison between exposure trials and real structure surveys. *Construction Building Materials* 113, 979–987. doi: 10.1016/j.conbuildmat.2016.03.156
- Patil, S. V., Rao, K. B., and Nayak, G. (2021). Influence of silica fume on mechanical properties and microhardness of interfacial transition zone of different recycled aggregate concretes. *Adv. Civil Eng. Materials* 10, 412–426. doi: 10.1520/acem20210011
- Pontes, J., Real, S., and Alexandre Bogas, J. (2023). The rapid chloride migration test as a method to determine the chloride penetration resistance of concrete in marine environment. *Construction Building Materials* 404. doi: 10.1016/j.conbuildmat.2023.133281
- Prusty, J. K., and Pradhan, B. (2023). Evaluation of durability and microstructure evolution of chloride added fly ash and fly ash-GGBS based geopolymer concrete. *Construction Building Materials* 401. doi: 10.1016/j.conbuildmat.2023.132925
- Pu, Y., Li, L., Wang, Q., Shi, X., Luan, C., Zhang, G., et al. (2021). Accelerated carbonation technology for enhanced treatment of recycled concrete aggregates: A state-of-the-art review. *Construction Building Materials* 282. doi: 10.1016/j.conbuildmat.2021.122671

- Qian, R. S., Li, Q., Fu, C. Q., Zhang, Y. S., Wang, Y. X., and Jin, X. Y. (2023). Atmospheric chloride-induced corrosion of steel-reinforced concrete beam exposed to real marine-environment for 7 years. *Ocean Eng.* 286. doi: 10.1016/j.oceaneng.2023.115675
- Quattrone, M., Cazacliu, B., Angulo, S. C., Hamard, E., and Cothenet, A. (2016). Measuring the water absorption of recycled aggregates, what is the best practice for concrete production? *Construction Building Materials* 123, 690–703. doi: 10.1016/j.conbuildmat.2016.07.019
- Shen, X., Liu, Q., Hu, Z., Jiang, W., Lin, X., Hou, D., et al. (2019). Combine ingress of chloride and carbonation in marine-exposed concrete under unsaturated environment: A numerical study. *Ocean Eng.* 189. doi: 10.1016/j.oceaneng.2019.106350
- Song, X., Kong, Q., and Liu, X. (2007). Experimental study on chloride threshold levels in OPC. *Tumu Gongcheng Xuebao/China Civil Eng. J.* 40, 59–63.
- Sua-iam, G., and Makul, N. (2024). Characteristics of non-steady-state chloride migration of self-compacting concrete containing recycled concrete aggregate made of fly ash and silica fume. *Case Stud. Construction Materials* 20. doi: 10.1016/j.cscm.2024.e02877
- Sun, C., Yuan, L., Zhai, X., Qu, F., Li, Y., and Hou, B. (2018). Numerical and experimental study of moisture and chloride transport in unsaturated concrete. *Construction Building Materials* 189, 1067–1075. doi: 10.1016/j.conbuildmat.2018.08.158
- Tam, V. W. Y., Butera, A., Le, K. N., and Li, W. (2020). Utilising CO2 technologies for recycled aggregate concrete: A critical review. *Construction Building Materials* 250. doi: 10.1016/j.conbuildmat.2020.118903
- Titi, H. H., and Tabatabai, H. (2018). Effect of coarse aggregate type on chloride ion penetration in concrete. *Construction Building Materials* 162, 871–880. doi: 10.1016/j.conbuildmat.2018.01.090
- Vintimilla, C., Etxeberria, M., and Li, Z. Y. (2023). Durable structural concrete produced with coarse and fine recycled aggregates using different cement types. *Sustainability* 15. doi: 10.3390/su151914272
- Wally, G. B., Larrossa, M., Pinheiro, L., Real, M., and Magalhães, F. C. (2023). 6-month evaluation of concrete aging factor using chloride migration test: Effects of binder type and w/b ratio. *Materialia* 30. doi: 10.1016/j.mtla.2023.101841
- Wang, C., Xiao, J., Zhang, G., and Li, L. (2016). Interfacial properties of modeled recycled aggregate concrete modified by carbonation. *Construction Building Materials* 105, 307–320. doi: 10.1016/j.conbuildmat.2015.12.077
- Wu, L., Xiang, Z., Jiang, H., Liu, M., Ju, X., and Zhang, W. (2022). A review of durability issues of reinforced concrete structures due to coastal soda residue soil in China. *J. Mar. Sci. Eng.* 10. doi: 10.3390/jmse10111740
- Wu, L. J., Zhang, W. X., Jiang, H., Ju, X. L., Guan, L., Liu, H. C., et al. (2023). Synergistic effects of environmental relative humidity and initial water content of recycled concrete aggregate on the improvement in properties via carbonation reactions. *Materials* 16. doi: 10.3390/ma16155251
- Xia, R. L., Jia, C., Liu, C. Y., Liu, P. Y., and Zhang, S. M. (2023). Non-uniform corrosion characteristics of the steel pipe pile exposed to marine environments. *Ocean Eng.* 272. doi: 10.1016/j.oceaneng.2023.113873
- Xiaoping, Z., Weiliang, J., and Baojian, Z. (2016). Durability design method of concrete structures under chlorine environment. *J. Build. Mat.* 19, 3.
- Xu, Q. H., Shi, D. D., and Shao, W. (2019). Service life prediction of RC square piles based on time-varying probability analysis. *Construction Building Materials*. 227. doi: 10.1016/j.conbuildmat.2019.116824
- Xuan, D., Zhan, B., and Poon, C. S. (2016b). Development of a new generation of eco-friendly concrete blocks by accelerated mineral carbonation. *J. Cleaner Production* 133, 1235–1241. doi: 10.1016/j.jclepro.2016.06.062
- Yang, S. Q., Gu, M. J., Lin, H. Y., and Gong, Y. (2023). Property improvement of recycled coarse aggregate by accelerated carbonation treatment under different curing conditions. *Sustainability* 15. doi: 10.3390/su15064908
- Zhang, Y., Wu, S., Ma, X., Fang, L., and Zhang, J. (2022). Effects of additives on water permeability and chloride diffusivity of concrete under marine tidal environment. *Construction Building Materials* 320. doi: 10.1016/j.conbuildmat.2021.126217
- Zhang, J., Zhou, X., Zhang, Y., Wang, M., and Zhang, Y. (2020). Stable process of concrete chloride diffusivity and corresponding influencing factors analysis. *Construction Building Materials* 261. doi: 10.1016/j.conbuildmat.2020.119994